frontiers in Earth Science

ORIGINAL RESEARCH
published: 21 January 2022
doi: 10.3389/feart.2021.823161

The Process of Tectonic Inversion and Disintegration in the Dasanjiang Unified Basin, Northeast China: Constraint From Low-Temperature Thermochronology

Yunpeng Zhang[1,2], Yan Tang[3], Shan Wang[4], Wang Guo[1], Wei Han[1], Shangwei Ma[1], Zhengyang He[1] and Jianye Ren[5]**

[1]Xi'an Center of China Geological Survey, Shaanxi, China, [2]Shaanxi Key Laboratory of Petroleum Accumulation Geology, Shaanxi, China, [3]School of Earth Science and Resources, Chang'an University, Shaanxi, China, [4]PetroChina Research Institute of Petroleum Exploration and Development, Beijing, China, [5]College of Marine Science and Technology, China University of Geosciences, Wuhan, China

OPEN ACCESS

Edited by:
Xiubin Lin,
Zhejiang University, China

Reviewed by:
Fengqi Zhang,
Zhejiang University, China
Jianping Zhou,
Ocean University of China, China

***Correspondence:**
Yan Tang
tangyan2011@chd.edu.cn
Jianye Ren
jyren@cug.edu.cn

Specialty section:
This article was submitted to Structural Geology and Tectonics, a section of the journal Frontiers in Earth Science

Received: *26 November 2021*
Accepted: *29 December 2021*
Published: *21 January 2022*

Citation:
Zhang Y, Tang Y, Wang S, Guo W, Han W, Ma S, He Z and Ren J (2022) The Process of Tectonic Inversion and Disintegration in the Dasanjiang Unified Basin, Northeast China: Constraint From Low-Temperature Thermochronology. Front. Earth Sci. 9:823161. doi: 10.3389/feart.2021.823161

The Dasanjiang basin group in Northeast China contains more than ten Mesozoic–Cenozoic sedimentary basins. Much evidence shows that they were a unified large-scale depression lacustrine basin in the Early Cretaceous; however, destruction processes and mechanisms after the formation of the unified lacustrine basin are some of the key issues restricting basic research and oil and gas exploration in the Dasanjiang area. In this study, we carried out low-temperature thermochronology and thermal history inversion on samples from the main basins in the Dasanjiang area to finely restore the destruction process of the unified basin. The results show that since the Early Cretaceous, the Dasanjiang area has experienced three major positive tectonic inversions: 100 Ma ~ 90 Ma, 73 Ma ~ 40 Ma, and 23 Ma ~ 5 Ma. The unified basin was destroyed by compression and uplift and gradually disintegrated. The basin gradually changed from initial unified evolution to differential evolution and finally formed the isolated appearance of each basin. The aforementioned three-stage positive tectonic inversion time limits basically corresponded to the changing periods in the movement direction, subduction angle, and movement speed of the paleo–Pacific Ocean plate. It is believed that the movement and reorganization events of the plates on the Pacific side dominated the formation, destruction, and disintegration of the Dasanjiang prototype basin, which was the main dynamic mechanism of the tectonic evolution of the Mesozoic and Cenozoic basins in the study area and Northeast China.

Keywords: Dasanjiang area in Northeast China, low-temperature thermochronology, Mesozoic–Cenozoic basin, tectonic-thermal evolutionary processes, tectonic inversion

INTRODUCTION

The Dasanjiang basin group is located in the eastern part of Heilongjiang Province, China, and includes Sanjiang, Boli, Jixi, Hulin, and other Mesozoic–Cenozoic sedimentary basins. In recent years, different scholars have done much research on the stratigraphic division and correlation, and sequence stratigraphic framework (Sha, 2002; Sun and David, 2002; Li and Yang, 2003; Ren et al., 2005; He, 2006; Zhang et al., 2017), provenance analysis (Wen et al., 2008; Zhang F. Q. et al., 2011; Wang et al., 2012; Zhang F.-Q. et al., 2012; Zhao et al., 2012; Zhang F.-Q et al., 2015), subsidence rate and basin history (Cao et al., 2001; Wu et al., 2007), tectonic characteristics and basin evolution (Gao, 2007; He et al., 2008; Shi et al., 2008; Sun et al., 2008; He et al., 2009; Zhang Y. P. et al., 2012; Yang, 2013; Zhou et al., 2020), and basement characteristics and deep faults (Zhang and Shi, 1992; Uchimura et al., 1996; Ren et al., 2002; Zhang et al., 2005) of the Dasanjiang area. However, due to the transformation of various basins by multistage tectonic movements, the degree of research of each basin varies differently. Previous researchers still have differences in understanding the prototype of the basin. Some scholars have studied the nature of basin boundary faults, the time limit of volcanic activity in the basin, and the coupling relationship between uplift and subsidence. They have believed that these basins were a series of independent extensional fault basin groups in the Early Cretaceous (Liu et al., 2000; Zhang et al., 2004; Liu et al., 2011; Cao et al., 2013). Other scholars have tended to consider that the currently divided basins were a unified large-scale depression basin during the Early Cretaceous through the study of sedimentary facies, paleocurrent, heavy minerals, and earthquakes (He, 2006; Wen et al., 2008; Jia and Zheng, 2010; Fang et al., 2012; Xu et al., 2013; Zhang et al., 2016) and that they need to be studied as a whole.

Researchers have performed many studies on the prototype restoration of the Dasanjiang unified basin, but the time of disintegration and the destruction and transformation processes of the later unified basin are not clear, which directly affects the restoration of basin appearance, evaluation of source–reservoir–caprock combinations, and the understanding of hydrocarbon accumulation. In different periods of the Mesozoic and Cenozoic in this area (Wu et al., 2004), the fission track in low-temperature thermochronology carries rich information such as age, length, and distribution and is an important method for quantitatively and systematically studying the tectonic-thermal evolution of the basin (Gleadow et al., 1986a; Henry et al., 1996; Carter and Moss, 1999). Previous studies have been conducted on fission tracks in the Dasanjiang Basin and its adjacent areas, but most of them were based on outcrop samples (Chen et al., 1997; Huang et al., 1997; Han et al., 2008; Chen, 2016; Zhang, 2019; Zhao, 2020; Zhou et al., 2020). This study uses the low-temperature thermochronology analysis of outcrops and core samples, combined with the structural analysis of seismic profiles and thermal history simulation to quantitatively restore the time, episode, and scale of tectonic inversion after the formation of the unified basin, finely describing the damaged tectonic-thermal evolutionary process of the basin, and discusses the corresponding dynamic mechanisms. This study will help us deeply understand the evolutionary process and development mechanisms of Mesozoic–Cenozoic basins in Northeast China and provide reference for oil and gas exploration in the Dasanjiang area.

REGIONAL GEOLOGICAL BACKGROUND

Tectonic Setting

The Dasanjiang Basin group is located in eastern Heilongjiang Province, China (**Figure 1A**), and the regional tectonic location is situated in the eastern Central Asian Orogenic Belt. The basin is mainly distributed above the Bulieya–Jiamusi terrane and includes the adjacent area Songnen–Zhangguangcailing terrane, Xingkai terrane, and part of the Nadanhada terrane (**Figure 1B,C**) (Zhou et al., 2009). Since the Paleozoic, the area has been jointly affected by the paleo–Asian Ocean tectonic and circum-Pacific tectonic domains (Ren et al., 1999; Zhou et al., 2009; Zhang F. Q. et al., 2012; Zhou and Wilde, 2013; Zhang X. Z. et al., 2015). Before the Jurassic, it was mainly in the paleo–Asian Ocean tectonic domain. With the closure of the Mongolian-Okhotsk Ocean in the Middle and Late Jurassic and the subduction of the paleo-Pacific plate underneath the East Asian continent, the tectonic setting in eastern China changed significantly approximately 180 Ma (Zhao et al., 1994; Zheng et al., 1998; Safonova et al., 2009; Zhou et al., 2009; Zhang F.-Q. et al., 2015) and was generally subjected to compression, indicating that Northeast China had basically entered the evolutionary stage of the circum-Pacific tectonic domain (Ren et al., 1999; Zhou et al., 2009; Sun et al., 2013; Zhou and Wilde, 2013), and subduction in different directions of the paleo-Pacific plate dominated the evolutionary process of the basin. Therefore, the evolution of the basin in Northeast China was jointly affected by multiple tectonic events, including plate collage, Mongolia-Okhotsk Ocean closure, and the subduction of the Pacific plate during the Mesozoic–Cenozoic (Safonova et al., 2009; Sun et al., 2013; Zhou and Wilde, 2013; Zhang X. Z. et al., 2015; Li et al., 2019; Tian et al., 2019).

Stratigraphic Framework

The study area mainly contains Jurassic, Cretaceous, Paleogene, Neogene, and Quaternary strata, spanning two stratigraphic divisions. **Figure 2** shows the stratigraphic sedimentary sequences of the main basins in Dasanjiang area based on regional stratigraphic and biostratigraphic data, and previous stratigraphic division and correlation research results (Li et al., 2006). It shows that the Upper Jurassic strata in the Dasanjiang Basin are limited and only distributed in the Sanjiang Basin; the Lower Cretaceous strata are well developed in the whole area, except for the Didao Formation; the Upper Cretaceous strata are generally uplifted and eroded, and only remain in the Sanjiang, Hegang, Jixi, and Boli Basins due to regional tectonic activities; and the Paleogene and Neogene strata are mainly developed in the Tangyuan, Fangzheng, and Hulin Basin, while those in other basins are not complete.

Fracture System

The Dasanjiang Basin group is located in the superimposed area between the paleo–Asian Ocean tectonic domain and the

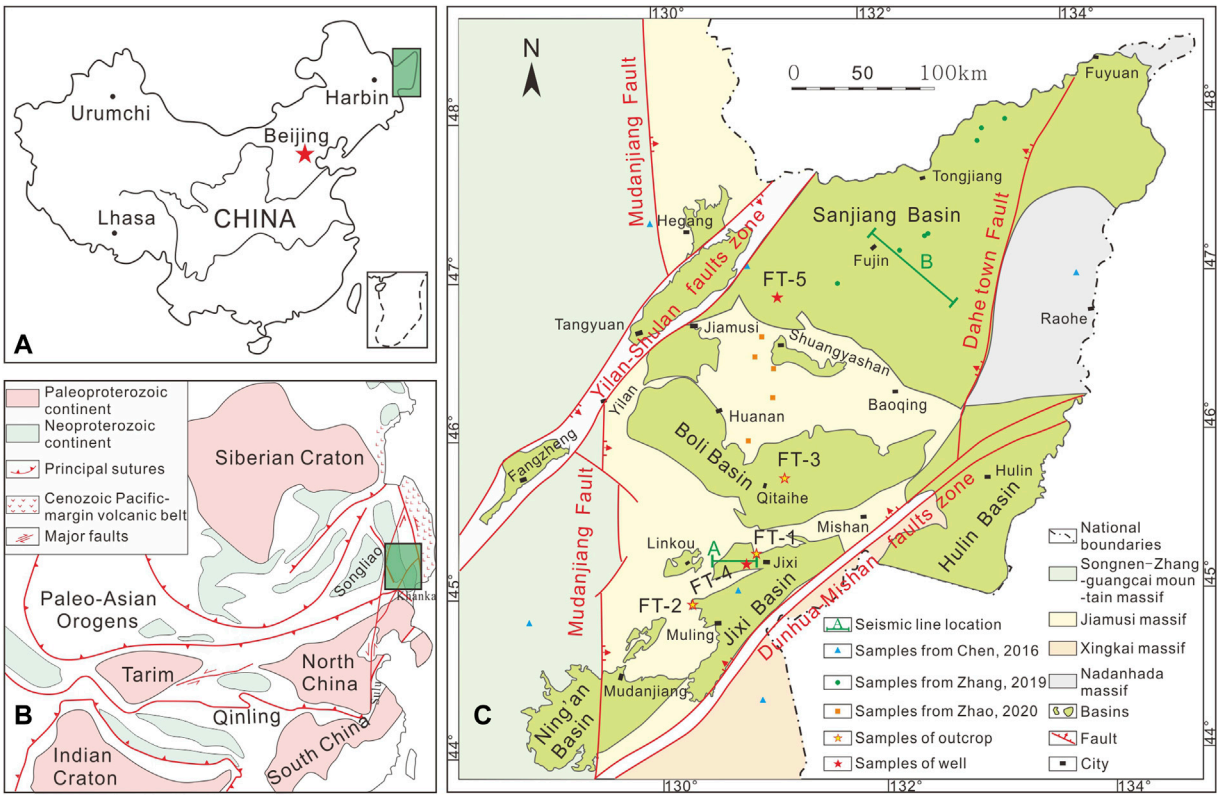

FIGURE 1 | (A) Schematic geographical location of Dasanjiang area (after the map of China). **(B)** Schematic tectonic map of Asia indicating the position of the Dasanjiang basin (modified after Safonova et al., 2009; Zhou et al., 2020). **(C)** Basin distribution and sampling location in Dasanjiang region, NE China (modified after Zhang Y. P. et al., 2012; Chen, 2016; Zhang et al., 2016; Zhang, 2019; Zhao, 2020; Zhou et al., 2020).

circum-Pacific tectonic domain, forming a complex fault system, including extensional faults, compressional faults, and strike–slip faults. These faults are characterized by a large number of fractures, most of which have multistage activity and often intersect with each other (He, 2006). This study focuses on the study of the failure process of the unified basin; therefore, the compressive structural fault system is discussed in detail. We have identified two-stage compression fracture systems in the Dasanjiang Basin since the Mesozoic through field geological investigation and seismic data interpretation. They are the late Early Cretaceous–early Late Cretaceous compression fracture system and the Late Cretaceous–early Paleogene compression fracture system.

Late Early Cretaceous–Early Late Cretaceous Compressional Fracture System

The fracture system in this period caused an obvious unconformity contact between the Upper Cretaceous and Lower Cretaceous strata or the upper strata in the region. It is mainly characterized by a series of clearly identified thrust faults in the seismic section, which mainly cut Lower Cretaceous strata, disappearing in the Upper Cretaceous strata, and the seismic reflection is characterized by truncation. The thrust faults are mostly developed in the Jixi Basin in this period (**Figure 3**). This series of nearly EW–NW trending thrust faults forms the boundary faults of the isolated basins in the Dasanjiang area. It can also be observed in the field outcrop that thrust faults cut the Muling and Chengzihe formations or that the basement was thrust upon the Muling and Chengzihe formations.

Late Cretaceous–Early Paleogene Compressional Fracture System

In the Late Cretaceous, the fault in the eastern part of the study area was characterized by the overall uplift of the basin, and the sedimentary strata in the earlier stage suffered erosion, especially the sedimentary strata during the Late Cretaceous, which only existed in local areas. The fault mainly cuts the Upper Cretaceous strata and almost disappears in Paleogene strata, and the seismic reflection is characterized by truncation. The fractures in this period are easier to identify on seismic profiles of the Qianjin depression in the Sanjiang Basin (**Figure 4**). The Upper Cretaceous strata suffered strong erosion after the uplift caused by compression, and then the Paleogene strata deposited over it. The seismic reflection showed an onlap above this interface and truncation below the interface. The Upper Cretaceous strata exposed in the field were seriously deformed by the faults of this period, and the Upper Cretaceous strata can be seen thrusting above the upper strata in many places.

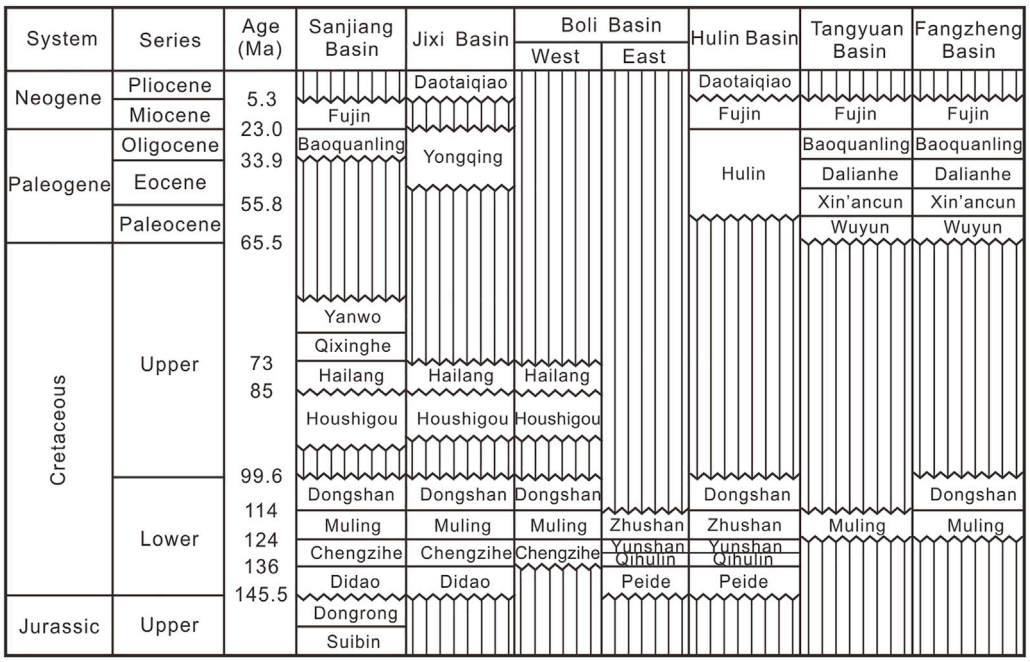

FIGURE 2 | Stratigraphic sedimentary sequences of major basins in Dasanjiang area, NE China (modified after Meng, 2007; Zhang and Ma, 2010; Zhang F. Q. et al., 2012; Zhang et al., 2016; Zhou et al., 2020). Zig-zag line: erosional unconformity.

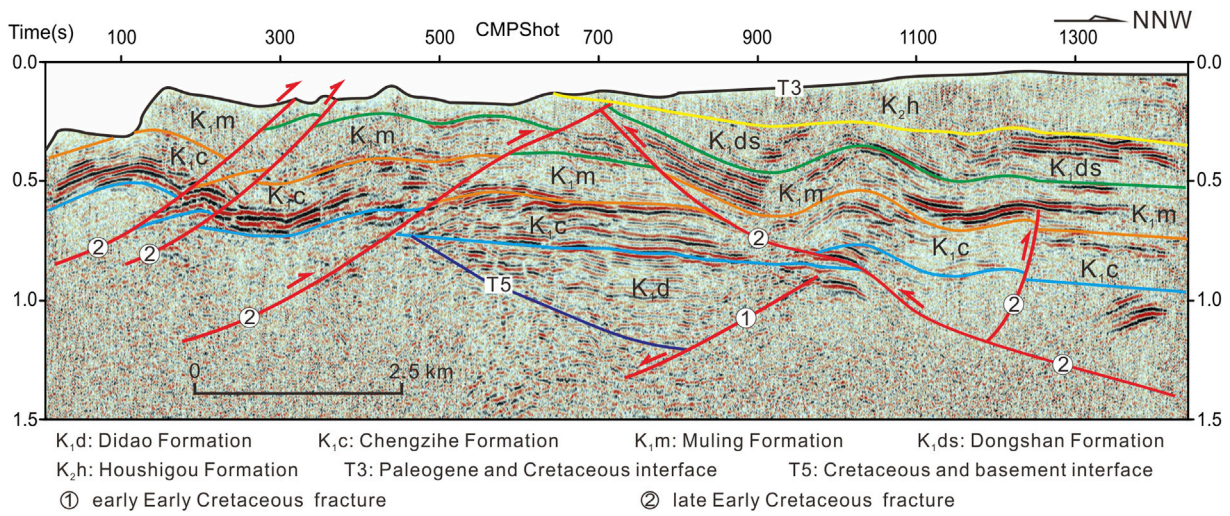

FIGURE 3 | Seismic reflection characteristics of compressional faults from late Early Cretaceous to early Late Cretaceous (Southern Jixi basin). Data from the project research team.

SAMPLES AND METHOD

Sampling

This study focuses on the tectonic evolutionary process of the destruction of the unified lacustrine basin formed by the Chengzihe Formation and Muling Formation in the Early Cretaceous. Therefore, samples were collected mainly in these two formations. We collected samples from the Didao Formation at the bottom of the Chengzihe Formation and Dongshan Formation at the top of the Muling Formation to ensure that the samples contained as much multistage tectonic information as possible and that the simulation results were more reliable. In this study, five fresh sandstone samples from the Jixi, Boli, and Sanjiang Basins were newly added on the basis of previous work, including three outcrop samples and two core samples. The sampling

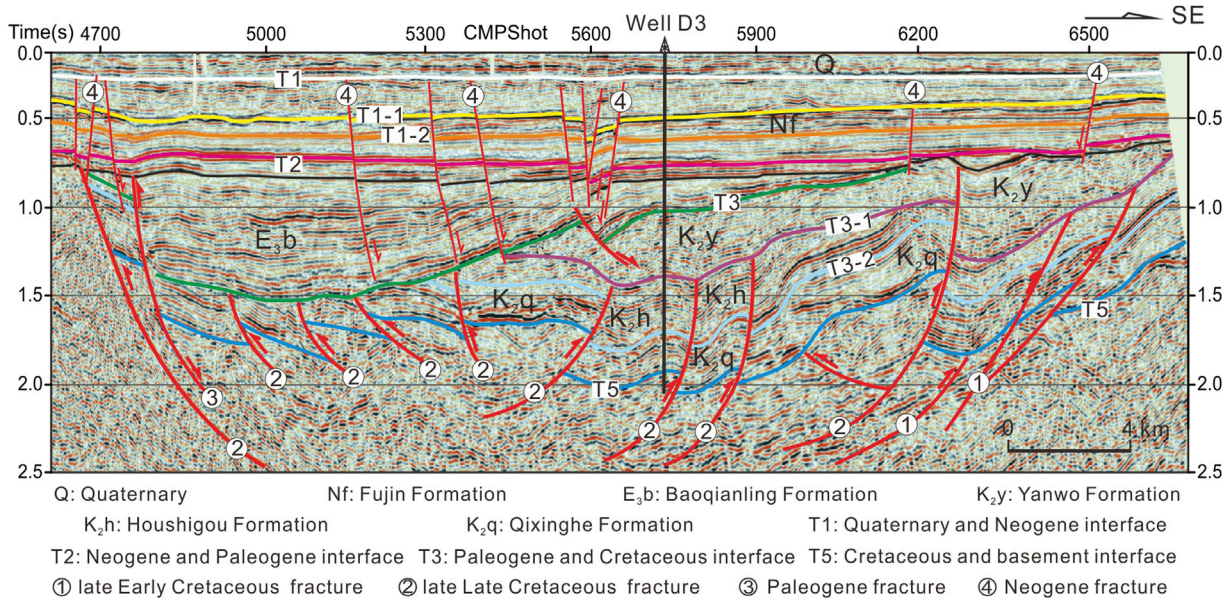

FIGURE 4 | Seismic reflection characteristics of compressional faults from late Late Cretaceous to early Paleogene (Qianjin depression of Sanjiang basin). Data from the project research team, and the strata calibration of the well (modified after Zhang F.-Q. et al., 2015).

TABLE 1 | Sample information of Dasanjiang area, NE China.

Sample number	Sampling location	Elevation (m)	Sample properties	Lithology	Sampling horizon	GPS
FT-1	Jixi city	219	Outcrop sample	Sandstone	K_1ch	N45°19′31.9″, E130°50′39.4″
FT-2	Jixi city	337	Outcrop sample	Sandstone	K_1m	N45°07′42.5″, E130°43′10.9″
FT-3	Qitaihe city	260	Outcrop sample	Sandstone	K_1ds	N45°46′29.3″, E130°52′14.9″
FT-4	Ji 6 well	−950	Core sample	Fine sandstone	K_1m	—
FT-5	Bincan 1 well	−3,020	Core sample	Gritstone	K_1d	—

location is shown in **Figure 1**, and the sample information is listed in **Table 1**.

The FT-1 sample was collected from a channel sandstone in the Chengzihe Formation on the north bank of the Muling River in Jixi city, and the FT-2 sample was collected from a lenticular sandstone in the Muling Formation beside Provincial Highway 206 in Jixi city. Generally, these two sections are dominated by delta plain subfacies, with continuous sedimentation and undeveloped faults. The FT-3 sample was collected from a sandstone in Dongshan Formation next to Provincial Highway 308 in Qitaihe city. There is a parallel unconformity contact between the Dongshan Formation and Muling Formation in this section. Breccia tuff can be seen in the Dongshan Formation, but the sampling location is located in the upper part and was not affected by thermal anomalies. The FT-4 sample was collected from a channel sandstone in the Ji 6 Well, and the vertical direction is mainly composed of continuous fan delta facies and lacustrine facies. The FT-5 sample was collected from a channel sandstone in the Bincan 1 Well. Andesite developed approximately 15 m below it. Therefore, the sample was not affected by magmatic activity.

Fission Track Experimental Procedures

The crushing of samples and the selection of apatite particles were performed at Chengxin Geology Service Co., Ltd, Langfang, Hebei Province, China, and the testing of the samples was conducted at the Institute of High Energy Physics Chinese Academy of Sciences. In the preparation of apatite samples, the apatite particles were first placed on glass slides, fixed with epoxy resin, ground and polished, and then etched at 25°C with 7% HNO_3 for 30 s to reveal the spontaneous tracks. An external detector was used for aging, and low-uranium muscovite was used as an external detector, combined with the samples and CN5 standard uranium glass, and placed in the nuclear reactor for irradiation. The neutron flux was 1×10^{16} cm^{-2}. After irradiation, the low-uranium muscovite was etched in 40% HF at 25°C for 20 s to reveal the induced tracks (Bellemans et al., 1994; Yuan et al., 2001).

Using the nuclear track automatic measurement system of Autoscan company, in accordance with the procedure suggested by Green (1986), a cylinder surface parallel to the c-axis was selected to measure the spontaneous track density, induced track density, and horizontal closed track length (Gleadow et al., 1986a; Gleadow et al., 1986b). The age was calculated

TABLE 2 | Fission track analysis results of samples.

Sample number	Sampling horizon	Grain number	ρ_s (10^5/cm^2) (Ns)	ρ_i (10^5/cm^2) (Ni)	ρ_d (10^5/cm^2) (N)	P (χ2) (%)	Central age (Ma) (±1σ)	Pooled age (Ma) (±1σ)	L (μm) (N)
FT-1	K_1c	12	2.471 (385)	12.920 (2013)	22.148 (10,405)	5.5	77 ± 7	82 ± 6	12.3 ± 2.2 (72)
FT-2	K_1m	27	3.996 (988)	19.464 (4,812)	17.565 (10,405)	0	66 ± 5	70 ± 4	12.2 ± 2.2 (106)
FT-3	K_1ds	28	1.747 (294)	6.833 (1150)	18.064 (10,405)	14.7	87 ± 8	89 ± 7	13.2 ± 2.1 (59)
FT-4	K_1m	28	3.685 (989)	23.998 (6,440)	16.669 (10,405)	0	49 ± 4	50 ± 3	11.9 ± 1.9 (102)
FT-5	K_1d	33	0.618 (168)	23.793 (6,467)	17.565 (10,405)	0	8.1 ± 1.2	8.9 ± 0.8	10.4 ± 2.2 (11)

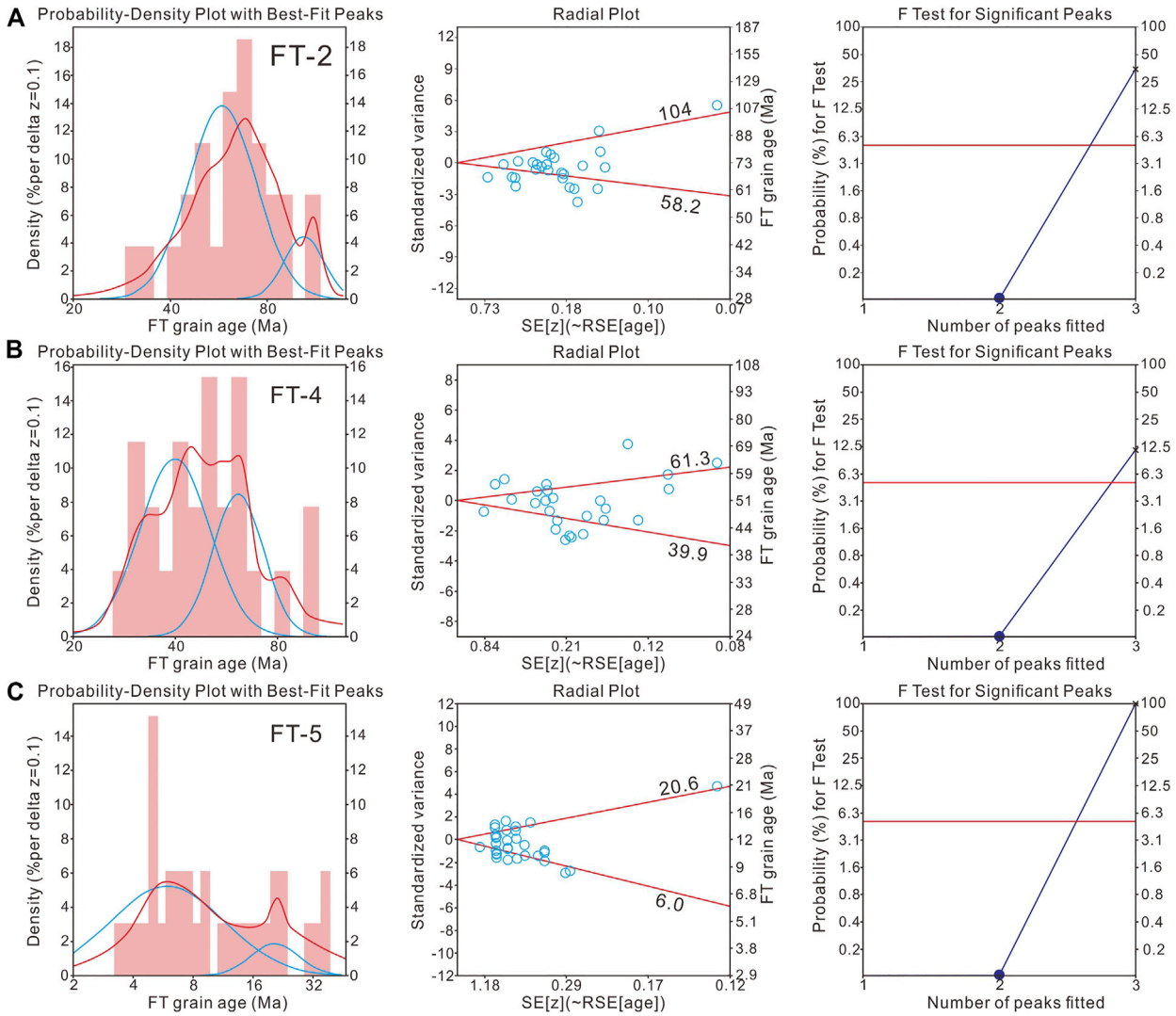

FIGURE 5 | Decomposition results of apatite fission track center age of the sample. The left picture shows the single-particle age distribution histogram, in which the red line is the fitting curve of the single-particle age histogram, and the blue line is the fitting curve of the two age-groups after decomposition. The middle picture is a single-particle age radar chart, in which the red line is the age of the decomposed age-group. The right picture is the P (F) test chart.

according to the Zeta constant method recommended by IUGS and the standard fission track age equation (Hurford and Green, 1983). The Zeta constant of apatite was 389.4 ± 19.2 in this study. The fission tracks of minerals were measured under a high-power microscope with a high-precision optical microscope.

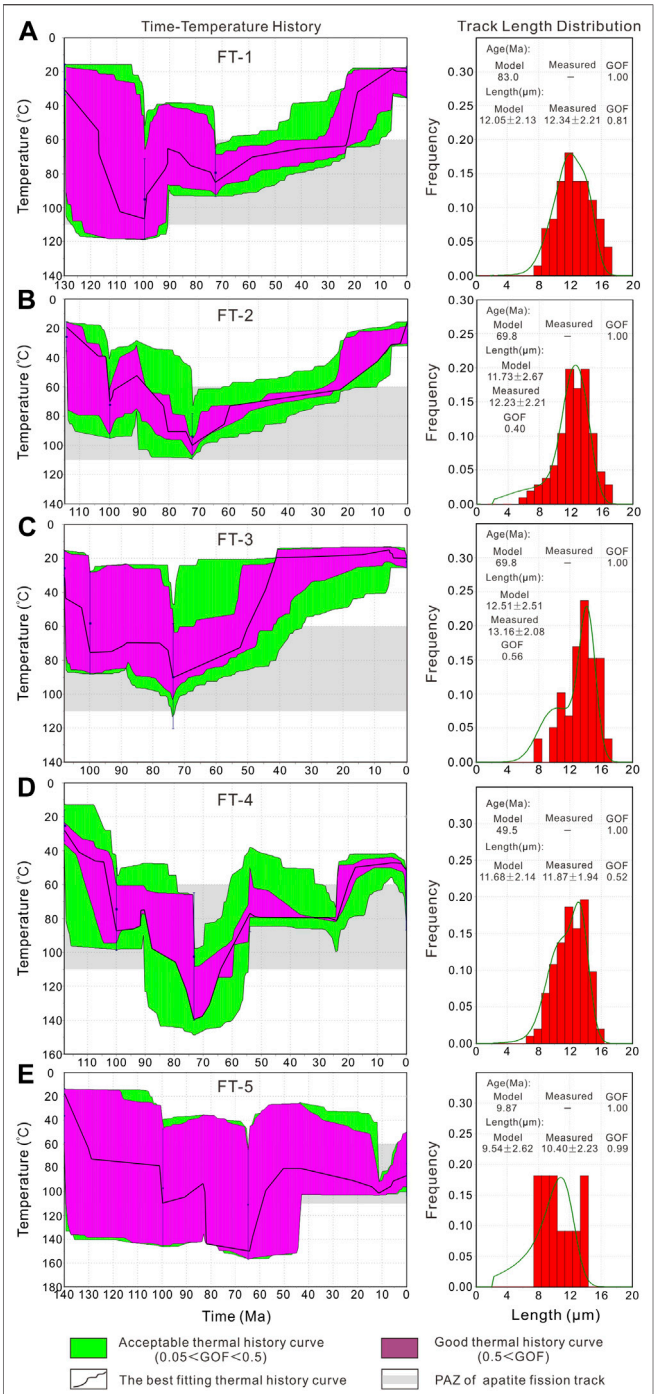

FIGURE 6 | Simulation results of time-temperature history in the Dasanjiang area. In the left picture, the green line indicates the acceptable thermal history path, the pink line indicates the good thermal history path, the black line indicates the optimal thermal history path, the blue line indicates the constraints of thermal history modeling, and the gray box indicates the annealing of apatite belt. In the right picture, the red column indicates the confined fission track length distribution of the apatite and the green line indicates the result of the fitting.

RESULTS

Results of Fission Track Analysis

The confined fission track length of the five apatite samples tested ranged from 10.4 ± 1.1 μm to 13.2 ± 2.1 μm, and the fission track age of the apatite ranged from 8.1 ± 1.2 Ma to 87 ± 8 Ma (**Table 2**). The fission track ages of all apatite samples were younger than their stratigraphic ages, indicating that the samples had experienced different degrees of tectonic-thermal events. The distribution of a single-particle age was tested by P (χ^2) values (Galbraith, 1981; Green, 1981; Galbraith and Laslett, 1993). The results showed that only two samples, FT-1 and FT-3, had a P (χ^2) value greater than 5%, indicating that the single-particle age belonged to the same age-group, reflecting the record of the last thermal event, and the pooled age of the sample was preferred, which was usually equal to the central age. Other samples had a P (χ^2) value less than 5%, indicating that the single-particle age had a mixed age, reflecting the ages from different thermal events. The age-group needed to be decomposed into multiple individual age-groups according to the characteristics of the Poisson distribution in the application. The age after decomposition was used.

BinomFit software (Brandon, 1992) was used to decompose the age-group of samples with a P (χ2) value less than 5%. Finally, the age-groups of FT-2 were decomposed into 58.2 Ma and 104 Ma, FT-4 into 39.9 Ma and 61.3 Ma, and FT-5 sample into 6.0 Ma and 60.6 Ma (**Figure 5A–C**). The age-groups of samples after decomposition passed the P (F) testing, showing that the decomposition results of the age-group of samples with mixed ages are credible.

Results of Thermal History Modeling

HeFTy software was used for thermal history inversion modeling, and four constraints were set according to the geological background of the region. The starting time was set to be less than the age of the lower boundary of this formation according to the sampling position, and the temperature was set to approximately 15°C, which was the same as the ancient surface temperature; the end time was set to approximately 0 Ma, and the temperature of the outcrop sample was set to approximately 20°C, which was the same as the current surface temperature (FT-1, FT-2, and FT-3). The temperature of the drilling sample was determined according to the current surface temperature, the geothermal gradient, and the sampling depth. The temperature of the FT-4 sample was set to 50 ± 5°C, and the temperature of the FT-5 sample was set to 105 ± 5°C. Data such as ancient surface temperature, ancient geothermal gradient, current surface temperature, current geothermal gradient, and stratigraphic age were from Meng (2007) and Zhou et al. (2020). There are obvious unconformities between the Upper Cretaceous and Lower Cretaceous strata and between the Cretaceous and Paleogene strata in the study area. Therefore, constraint conditions needed to be set. The development time of the unconformity between the Upper Cretaceous and Lower

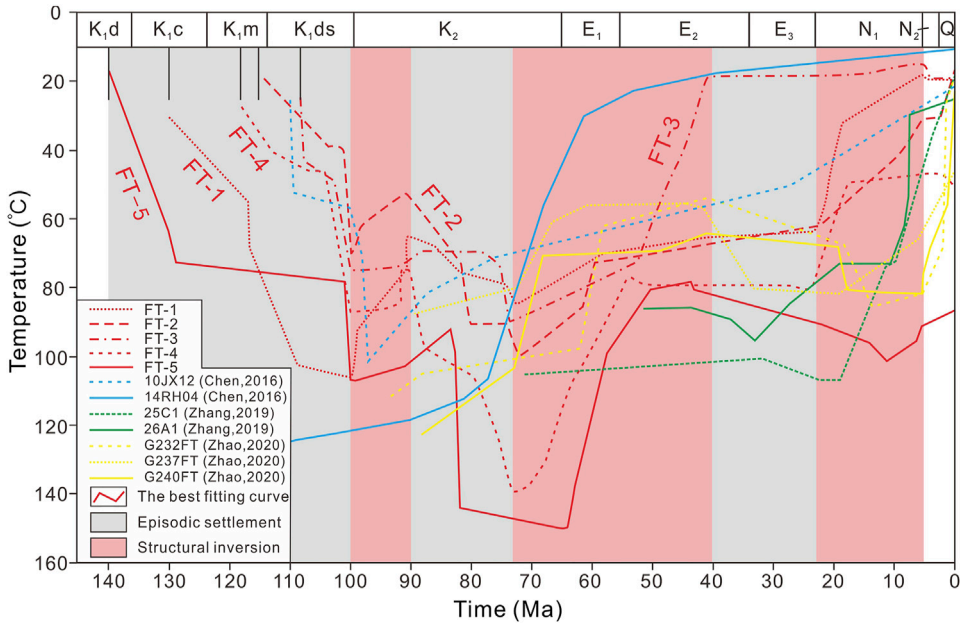

FIGURE 7 | Comprehensive analysis of tectonic-thermal evolution process of the Dasanjiang area. The lines of different colors and styles indicate the best thermal history path of the sample and the thermal history simulation results of predecessors (modified after Chen, 2016; Zhang, 2019; Zhao, 2020).

Cretaceous strata was set to 100 ± 5 Ma, the development time of the unconformity between the Cretaceous and Paleogene strata was set to 70 ± 5 Ma, and their temperature settings were based on the results of drilling burial history from Meng (2007) and Zhou et al. (2020). Afterward, HeFTy software was used to perform thermal history inversion, the annealing model used the Ketcham annealing model (Ketcham et al., 2000), and the simulation method used the Monte Carlo method (Ketcham et al., 2005). The number of fitting curves was set to 10,000, and the calculated ages and track length distributions were compared with the measured data. The modeled results were then categorized as good or acceptable according to the goodness of fit parameter, and finally, the optimal path was selected to represent the thermal history of the sample. **Figure 6** shows the simulation results of each sample as follows.

The simulation results of sample FT-1 were very good. The stratigraphic age of the sample was estimated to be 130 Ma, and the simulation age of the fission track was 83.0 Ma, the simulation track length was 12.05 ± 2.13 μm, and the length GOF value was 0.81. Its thermal history was mainly divided into the following stages: the first heating stage from 130 Ma to 100 Ma, in which the average heating rate was 2.52°C/Ma, and there was a rapid heating approximately 116 Ma; the first cooling stage from 100 Ma to 90 Ma, in which the average cooling rate was 4.1°C/Ma, and there were two rapid cooling events approximately 100 Ma and 90 Ma; the second heating stage from 90 Ma to 73 Ma, in which the average heating rate was 1.18°C/Ma; the second cooling stage from 73 Ma to 40 Ma, in which the average cooling rate was 0.61°C/Ma; the third heating stage from 40 Ma to 23 Ma, in which the average heating rate was 0.12°C/Ma and heating was slow; the third rapid cooling stage from 23 Ma to 5 Ma with an average cooling rate of 2.78°C/Ma, in which cooling was rapid; and after 5 Ma, there was a slow heating stage with little temperature change (**Figure 6A**).

The simulation results of sample FT-2 were normal. The stratigraphic age of the sample was estimated to be 115 Ma. The fission track age had mixed age characteristics. The simulation age was 69.8 Ma. The simulation length of the track was 11.73 ± 2.67 μm, and the length GOF value was 0.40. Its thermal history was mainly divided into the following stages: the first heating stage from 115 Ma to 100 Ma, in which the average heating rate was 3°C/Ma, of which 102 Ma ~ 100 Ma had an extremely rapid heating stage and the heating rate was approximately 15°C/Ma; the first cooling stage from 100 Ma to 90 Ma with an average cooling rate of 1.8°C/Ma; the second heating stage from 90 Ma to 73 Ma at the average heating rate of 2.82°C/Ma; the second cooling stage from 73 Ma to 60 Ma with an average cooling rate of 2.08°C/Ma, from 60 Ma to 23 Ma with an average cooling rate of 0.27°C/Ma, and from 23 Ma to 5 Ma with an average cooling rate of 1.72°C/Ma; and after 5 Ma, it has been in a cooling stage (**Figure 6B**).

The simulation results of sample FT-3 were good. The stratigraphic age of the sample was estimated to be 108 Ma. The simulation age based on fission track was 69.8 Ma. The simulation length of the track was 12.51 ± 2.51 μm, and the length GOF value was 0.56. Its thermal history was mainly divided into the following stages: the first rapid heating stage was from 108 Ma to 100 Ma with an average heating rate of 5.63°C/Ma; the first cooling stage was from 100 Ma to 88 Ma with an average cooling rate of 0.42°C/Ma; the second heating stage was from 88 Ma to 74 Ma with an average heating rate of 1.43°C/Ma, in which there was rapid heating approximately 75 Ma; the second cooling stage

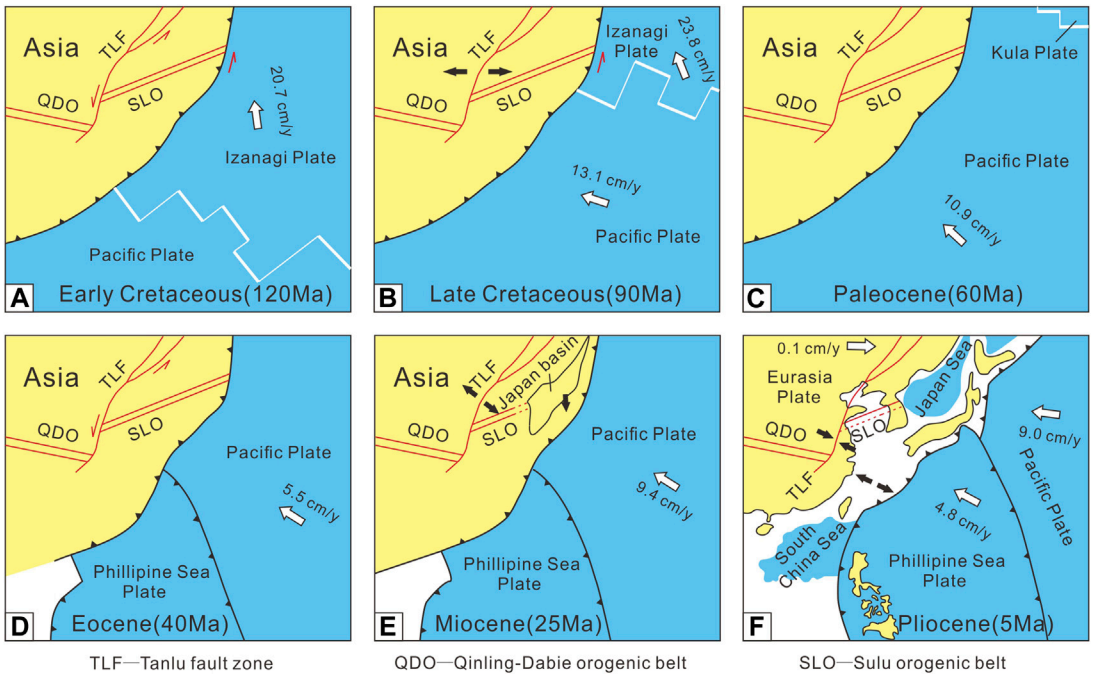

FIGURE 8 | Schematic diagram of plate activities evolution in Western Pacific since Cretaceous (modified after Maruyama et al., 1997; Zhu et al., 2004; Zhang X. Z. et al., 2015).

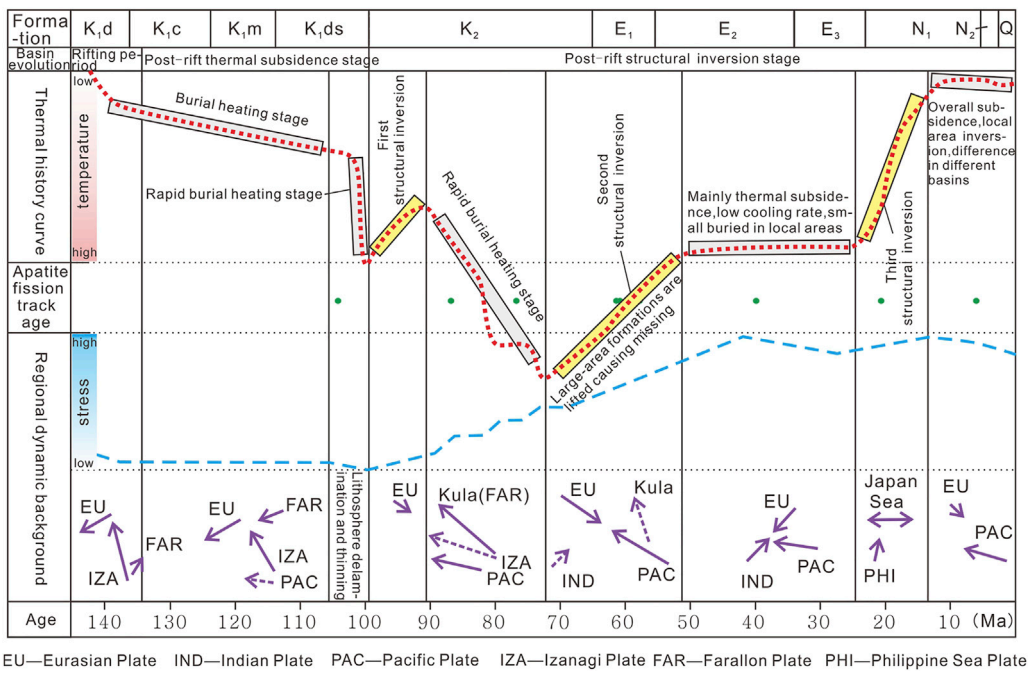

FIGURE 9 | Corresponding relationship between tectonic-thermal evolution and plates movement in the Dasanjiang unified basin. The red dashed line represents the comprehensive curve of the thermal history of the basin; the blue dashed line represents the magnitude of intraplate stress; the green dots represent the fission track age; the arrow represents the absolute movement direction of the plates, the line length represents the moving speed, and the dashed line represents the emergence or extinction of the plates. Plate activities data (modified after Engebretson et al., 1985; Northurp and Royden, 1995; Maruyama et al., 1997; Molnar and Stock, 2009; Copley et al., 2010).

was from 74 Ma to 33 Ma with an average cooling rate of 2.15°C/Ma, including three rapid cooling stages; the temperature did not change much afterward; and there was a small process of first cooling and then heating only during 15 Ma ~ 5 Ma (**Figure 6C**).

The simulation results of sample FT-4 were good. The stratigraphic age of the sample was estimated to be 118 Ma. The simulation based on the fission track was 49.5 Ma, the simulation length of the track was 11.68 ± 2.14 μm, and the length GOF value was 0.52. Its thermal history was mainly divided into the following stages: the first rapid heating stage was from 118 Ma to 100 Ma with an average heating rate of 3.33°C/Ma; the first cooling stage from 100 Ma to 90 Ma with an average cooling rate of 1.3°C/Ma; the second heating stage from 90 Ma to 74 Ma with an average heating rate of 3.31°C/Ma; the second cooling stage from 74 Ma to 54 Ma with an average cooling rate of 3.1°C/Ma; the third slow heating stage from 54 Ma to 24 Ma with an average heating rate of 0.1°C/Ma; the third cooling stage from 24 Ma to 5 Ma with an average cooling rate of 1.74°C/Ma, in which 24 Ma ~ 18 Ma was a rapid cooling stage; and after 5 Ma, it entered a heating stage with an average heating rate of 0.6°C/Ma (**Figure 6D**).

The simulation results of sample FT-5 were very good. The stratigraphic age of the sample was estimated to be 140 Ma. The simulation age based on fission track was 9.87 Ma. The simulation length of the track was 9.54 ± 2.62 μm, and the length GOF value was 0.99. Its thermal history was mainly divided into the following stages: the first heating stage from 140 Ma to 100 Ma with an average heating rate of 2.35°C/Ma, in which there were two rapid heating events in the period, 140 Ma ~ 130 Ma and 100 Ma; the first cooling stage from 100 Ma to 84 Ma with an average cooling rate of 1.25°C/Ma; the second heating stage from 84 Ma to 65 Ma with an average heating rate of 3.37°C/Ma, in which there was a rapid heating event approximately 84 Ma; the second cooling stage from 65 Ma to 45 Ma with an average cooling rate of 3.85°C/Ma; the third heating stage from 45 Ma to 11 Ma with an average heating rate of 0.65°C/Ma; and the third cooling stage after 11 Ma with an average cooling rate of 1.27°C/Ma (**Figure 6E**).

DISCUSSION

Temporal and Spatial Differences in the Tectonic Evolution of Dasanjiang Major Basins

It is generally considered that the thermal history of the basin is a direct reflection of the tectonic evolutionary history of the basin without the interference of abnormal thermal events. If the burial or uplift of the sample was entirely caused by tectonic movement, the sample experienced load subsidence and tectonic subsidence under the extension background. As the burial depth increases, the temperature of the sample was also increased. Similarly, when the structure reversed, the buried depth of the sample became smaller with the uplift of the stratum, and the temperature of the sample appeared to be cooling than before.

Combined with the thermal history simulation, paleogeothermal gradient, and other parameters, we can quantitatively calculate the subsidence or uplift amplitude and scale of the sample and restore the tectonic evolutionary history of the basin. The thermal history simulation of the samples from five different basins shows that they generally experienced three episodic evolutionary processes that included tectonic subsidence heating and three positive tectonic inversions uplift cooling processes since the Cretaceous (**Figure 7**), but there were differences in time and space in the specific evolutionary process.

During the formation period of the Dasanjiang unified basin, samples from all regions showed good synchronization. For example, the rapid subsidence and heating processes at the end of the Lower Cretaceous Dongshan Formation were recorded, and the maximum subsidence was up to 800 m (FT-4), corresponding to a development period of volcanic rocks in the Dongshan Formation (Zhang Y. P. et al., 2011; Zhang F.-Q. et al., 2015). The first positive tectonic inversion occurred in the basin 100 Ma ~ 90 Ma, with unified basin uplift and cooling, and only the cooling end time of the Sanjiang Basin sample (FT-1) was the latest (~ 84 Ma). During 90 Ma ~ 73 Ma, most areas were in a stage of subsidence heating, and the maximum subsidence was approximately 1280 m (FT-1). Only the Huanan area (G232FT, G237 FT, and G240 FT) was in a stage of uplift and cooling during this period (Han et al., 2008; Zhao, 2020), indicating that different areas of the unified basin began to show differences in the evolutionary process.

The second episode of positive tectonic inversion occurred in the study area at approximately 73 Ma and entered a stage of uplift and cooling. This period did not end until approximately 40 Ma at the latest, which comprehensively opened the prelude to the differential evolution of different regions. The evolutionary time and scale were different in different regions. For example, the Sanjiang Basin was first uplifted and then subsided, while the uplift cooling rate of the Jixi Basin was first fast and then slow. Even in the same basin, the evolutionary process of samples in different regions was different (Chen, 2016). During this period, a series of NE-trending thrust structures were formed, and the unified basin began to suffer compression damage (Zhang F. Q. et al., 2012; Zhou and Wilde, 2013; Zhang X. Z. et al., 2015).

The third episode of positive tectonic inversion that occurred approximately 23 Ma further exacerbated the segmentation degree of the Dasanjiang unified basin. The Jixi Basin in the west experienced rapid uplift and cooling, and the cooling rate of the Boli Basin in the middle was significantly lower than that of the Jixi Basin, while the Sanjiang Basin and its adjacent Huanan uplift (Zhao, 2020) manifested as a process of first heating and then cooling. This period was the main period for the formation and adjustment of the Dasanjiang Basin group. After 5 Ma, the appearance of the current basins was finally finalized under the influence of the regional structure.

Destruction and Disintegration Process of the Dasanjiang Unified Basin and Its Dynamic Mechanisms

Characteristics of Plate Movements

The Mesozoic and Cenozoic tectonic evolution of the East Asian continent was mainly controlled by the collision and convergence

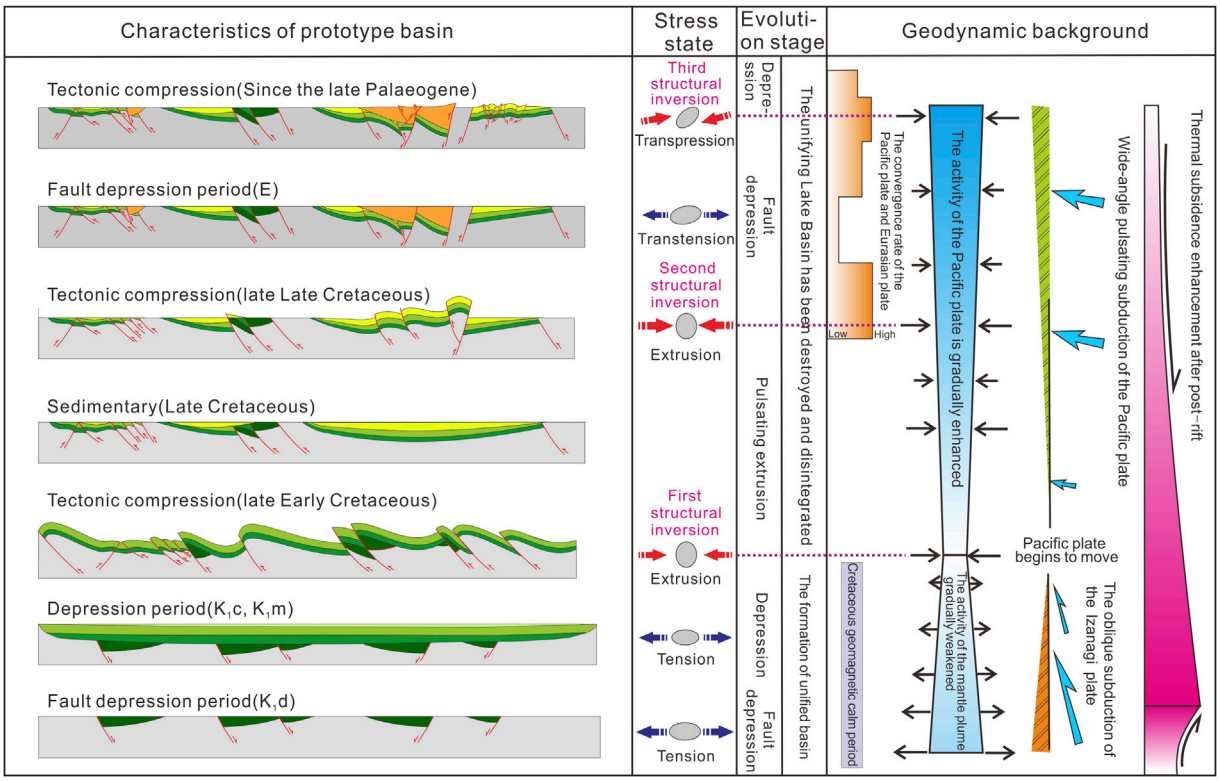

FIGURE 10 | Destruction and disintegration process and dynamic mechanism of the Dasanjiang unified basin. The gray ellipse indicates the stress state, the dark blue arrow indicates the extension state, and the red arrow indicates the extrusion state. The orange box color from light to dark indicates the convergence rate of the Pacific-Eurasian plate from low to high, the blue box color from light to dark indicates the activity of the mantle plume and the Pacific plate is gradually increasing, and the angle and size of the light blue arrow indicate the subduction rate and angle of the Izanagi plate and the Pacific plate, and the pink box color from light to dark indicates the thermal subsidence enhancement after post-rift.

of the Indo-European plate and subduction of the Pacific plate (Engebretson et al., 1985; Maruyama et al., 1997; Molnar and Stock, 2009; Copley et al., 2010). East China basically entered the evolutionary stage of the circum-Pacific tectonic domain after approximately 180 Ma (Ren et al., 1999; Zhou et al., 2009).

The Dasanjiang Basin group was in a buried heating stage during the entire Early Cretaceous. Due to the delamination and thinning of the lithosphere and changes in the subduction angle of the Izanagi plate (Ren et al., 2002; Wu et al., 2003; Sun et al., 2008), the magmatic activity occurred approximately 138 Ma and 104 Ma, respectively, causing the basin to be characterized by quick burial and heating (**Figure 7**). After 100 Ma, the subduction direction of the Pacific plate changed from NNW to NWW (Northrup and Royden, 1995; Maruyama et al., 1997; Song et al., 2015; Zhang et al., 2017) (**Figure 8A**), and the first positive tectonic inversion occurred in the whole area. The Lower Cretaceous strata thrust above the Upper Cretaceous strata, and the lower Upper Cretaceous strata are generally missing, forming an obvious angular unconformity between them (**Figure 3**). This stage lasted until approximately 90 Ma.

After 90 Ma, due to the Izanagi plate being incorporated into the Pacific plate (**Figure 8B**), the basin also showed multistage burial heating under the influence of pulsating subduction (**Figure 9**). Until approximately 73 Ma, with the gradual disappearance of the Kula plate, the Indian plate and Eurasian plate began soft collision and the subduction direction of the Pacific plate changed from NWW to NW. The basin suffered compression, and the second positive tectonic inversion occurred, forming an angular unconformity between the Cretaceous and Paleogene. The lower Paleogene strata are generally missing in the whole region, and this stage could have lasted until approximately 40 Ma (**Figure 8C,D**). Ren (2018) also identified the fault system formed by inversion compression in the deep layer of the Xihu Sag in the East China Sea.

After 40 Ma, the subduction direction of the Pacific plate in relation to the Eurasian plate changed to the NWW, and subduction began to retreat eastward (Zhou et al., 1995; Maruyama et al., 1997; Zhou and Wilde, 2013). During this period, the rigid collision between the Indian and Eurasian plates had less influence on the study area (Molnar and Stock, 2009; Copley et al., 2010), and the Dasanjiang Basin group basically entered a relatively calm stage of tectonics. Until 28 Ma, due to the back-arc spreading of the Japan Sea and the northward drifting of the Philippine Sea plate, which produced a large westward lateral pushing force, extensive compression of eastern China occurred, and the third episode of positive tectonic inversion occurred in the study area (**Figure 8E**), which lasted until approximately 10 Ma. Then the plate action

was relatively stable. The closure of the Sea of Japan and the collision between the Philippine Sea plate and the Japanese Islands caused small-scale tectonic subsidence and burial heating in the study area (**Figure 8F**).

The multistage evolution of the study area since the Cretaceous was the response and epitome of western Pacific plate activity. The plate kinematic reorganization events mainly expressed in the movement direction, and movement speed and subduction between the Eurasian and Pacific plates were the main dynamic mechanisms of tectonic evolution of the Mesozoic basin in Northeast China (**Figure 9**).

Destruction and Disintegration Processes of the Dasanjiang Unified Basin

Based on the comprehensive analysis of the kinematic characteristics of the positive tectonic inversion in the Dasanjiang Basin and the regional dynamic background, the processes of inversion destruction and disintegration after the formation of the Dasanjiang unified basin in the Early Cretaceous were reconstructed (**Figure 10**).

The first episode of positive tectonic inversion (late Early Cretaceous to early Late Cretaceous)

The dynamic background of eastern China changed in the late Early Cretaceous. At approximately 100 Ma, the subduction angle of the Pacific plate changed. At approximately 90 Ma, the subduction direction of the Izanaqi plate changed from NNW to NW, the subduction rate increased, and the force on the plate boundary from the Asian continent also changed from the original oblique subduction with slip to subduction. A strong collisional orogeny occurred on the edge of the East Asian continent, and the further compressional amalgamation occurred between the Nadanhada landmass and the East Asian continental margin. The Dasanjiang Basin was subjected to strong thrusting under a compressive stress in an NW-NWW direction. According to the age distribution of the fission tracks, the time of first compression inversion occurring in the Dasanjiang Basin was between 94.8 Ma and 87.7 Ma, and it had gradual inversion and uplift from west to east. This period of tectonic activity ended the sedimentation of the unified basin in the Early Cretaceous and caused its tectonic uplift with a maximum uplift of approximately 800 m. The unified basin was destroyed, forming the prototype of the present isolated basin.

The second episode of positive tectonic inversion (late Late Cretaceous to early Paleogene)

This episode of positive tectonic inversion occurred approximately 73 Ma and lasted for a long time until approximately 40 Ma. Since the beginning of the late Late Cretaceous, due to the expansion of the Pacific plate, the regional stress field changed. With continuous compression in NS direction, the relative movement of the Pacific plate and Eurasian plate gradually strengthened, and this tectonic activity showed pulsation from the simulation curve. The unconformities and missing strata between the Upper Cretaceous strata in the study area are best evidence for the pulsating subduction of the Pacific plate under Eurasia during this period. From the end of the Late Cretaceous to the beginning of the Paleogene, the entire Kula plate and Kula-Pacific ridge subducted beneath the Asian continent. The Dasanjiang Basin again suffered strong compression damage, with a maximum uplift of 1440 m, which was the strongest tectonic modification in the study area, and the shape of the basin was closer to its present appearance.

The third episode of the positive tectonic inversion (late Paleogene to early Neogene)

In the late Paleogene, the final subduction of the Kula-Pacific ridge caused the subduction direction of the Pacific plate to change from NW to NWW. Northeast China during this period was characterized by deep and large faults along an NNE direction, especially along the Yi-Shu and Dun-Mi fault zones, and rift basins were widely developed. From the late Paleogene to Neogene (~ 25 Ma), the convergence rate of the Eurasian-Pacific plate increased distinctly and the extension activity gradually decreased. Under the effect of local mantle convection and back-arc extension caused by subduction of the Pacific plate, the third positive tectonic inversion occurred in the study area. This tectonic activity had a great influence on the basins in the Yi-Shu and Dun-Mi fault zones, the whole study area was affected by tectonic compression and dextral strike–slip of the Yi-Shu and Dun-Mi faults, and the basin pattern was basically finalized.

In addition, since the Miocene, the tectonic evolutionary processes of the basins in the Dasanjiang area have been different (**Figure 7**), indicating that independent tectonic units were formed at this time. Although the subsequent tectonic activities had formed the final morphology of the basins, they had limited impact on the reformation of the Dasanjiang unified basin; therefore, they are not explicitly discussed. Moreover, due to limited data, all basins in this area were not analyzed individually, but they will be in future work.

CONCLUSIONS

In this study, we quantitatively restored the thermal history of the Dasanjiang area since the Cretaceous in Northeast China by using apatite fission track analysis and determined the time, period, and amplitude of tectonic activities experienced by the Dasanjiang unified basin. The results show that the Dasanjiang unified basin experienced three episodes of tectonic subsidence and heating, 140 Ma ~ 100 Ma, 90 Ma ~ 73 Ma, and 40 Ma ~ 23 Ma, and three episodes of positive tectonic inversion uplift and cooling, 100 Ma ~ 90 Ma, 73 Ma ~ 40 Ma, and 23 Ma ~ 5 Ma. The maximum heating rate and cooling rate were 5.63°C/Ma and 4.1°C/Ma, respectively, and the maximum subsidence and uplift were approximately 1280 m and 1440 m, respectively.

The detailed reconstruction of the tectonic-thermal evolutionary process shows that these three episodes of tectonic compression inversion were the main driving force for the destruction and disintegration of the Dasanjiang unified basin, which also led to the evolution of the basins in

the Dasanjiang area from early synchronization to late differentiation. The period of positive tectonic inversions basically corresponded to the period of changes in the movement direction, subduction angle, and movement speed of the plate on the Pacific side. We believe that the movement reorganization events of the plate on the Pacific side dominated the formation, destruction, and disintegration of the Dasanjiang prototype basin, which were the main dynamic mechanisms of tectonic evolution in the study area and in Northeast China.

DATA AVAILABILITY STATEMENT

The original contributions presented in the study are included in the article/supplementary material; further inquiries can be directed to the corresponding authors.

AUTHOR CONTRIBUTIONS

YZ, JR, and YT conceived the idea and did the fieldwork. SW, WG, WH, SM, and ZH prepared the samples and conducted the experiments. SW, WG, WH, and SM contributed to the data analysis and thermal history simulation. YT, and JR discussed. YZ interpreted the data and wrote the manuscript. All authors contributed to the revision of the text.

FUNDING

This study was supported by Open Fund of Shaanxi Key Laboratory of Petroleum Accumulation Geology (Grant No: PAG-202002), National Natural Science Foundation of China (Grant No: 41772109), and National Key Research and Development Program of China (Grant No: 2021YFA0719003).

ACKNOWLEDGMENTS

We thank Dr. Shengming Tang for help in decomposing age, and Zhang Fengqi, Xueqin Zhao, Sun Mingdao, and other members of the research team of Zhejiang University for help in seismic profile analysis. Constructive reviews by the two reviewers and editorial work by Xiubin Lin are gratefully appreciated.

REFERENCES

Bellemans, F., De, C. F., and Van, D. H. P. (1994). Composition of SRM and CN U-Doped Glasses: Significance for Their Use as thermal Neutron Fluence Monitors in Fission Track Dating. *Radiat. Meas.* 24, 153–160.

Brandon, M. T. (1992). Decomposition of Fission-Track Grain-Age Distributions. *Am. J. Sci.* 292, 535–564. doi:10.2475/ajs.292.8.535

Cao, C. R., Kirillova, G. L., Cao, H. S., Sorokin, A. P., Kaplun, V. B., Qu, Y., et al. (2013). Structure and Evolution of the Sunwu-Jiayin basin in NE China and its Relation to the Zeya-Bureya basin in the Far East of Russia. *Russ. J. Pac. Geol.* 7 (6), 431–440. doi:10.1134/s1819714013060055

Cao, C. R., Liu, Z. H., and Wang, D. P. (2001). The Structure Features and the Movement Regularity of Fault Blocks in Hulin basin, East Heilongjiang Province. *J. Changchun Univ. Sci. Technol.* 31, 304–344. (in Chinese with English abstract).

Carter, A., and Moss, S. J. (1999). Combined Detrital-Zircon Fission-Track and U-Pb Dating: a New Approach to Understanding Hinterland Evolution. *Geol* 27, 235–238. doi:10.1130/0091-7613(1999)027<0235:cdzfta>2.3.co;2

Chen, D. X. (2016). *Mesozoic-Cenozoic Tectonic Evolution and Low Temperature Thermochronological Study of Eastern Heilongjiang, NE China*. dissertation/doctor's thesis. Hangzhou: Zhejiang University. in Chinese with English abstract.

Chen, Z. N., Chen, F. J., and Dong, Y. (1997). Thermal History Analysis of Yanji basin. *Oil Gas Geology.* 18, 165–170. in Chinese with English abstract.

Copley, A., Avouac, J.-P., and Royer, J.-Y. (2010). India-asia Collision and the Cenozoic Slowdown of the Indian Plate: Implications for the Forces Driving Plate Motions. *J. Geophys. Res.* 115, B03410. doi:10.1029/2009jb006634

Engebretson, D. C., Cox, A., and Gordon, R. G. (1985). Relative Motions between Oceanic and Continental Plates in the Pacific Basin. *Geol. Soc. Am. Spe. Paper.* 206, 1–60. doi:10.1130/spe206-p1

Fang, S., Zhang, P. Z., Liu, Z. J., Liu, J. P., and Tang, J. (2012). Sedimentation Features and its Evolution since Cretaceous in the South of Eastern Sanjiang Basin. *J. Jilin Univ. (Earth Sci. Ed.* 42, 66–76. in Chinese with English abstract.

Galbraith, R. F., and Laslett, G. M. (1993). Statistical Models for Mixed Fission Track Ages. *Nucl. Tracks Radiat. Measurements* 21, 459–470. doi:10.1016/1359-0189(93)90185-c

Galbraith, R. F. (1981). On Statistical Models for Fission Track Counts. *Math. Geology.* 13, 471–478. doi:10.1007/bf01034498

Gao, C. W. (2007). *Late Mesozoic Tectonic Evolution and Prototype of Suibin Depression in Sanjiang basin*. dissertation/doctor's thesis. Hangzhou: Zhejiang University. in Chinese with English abstract.

Gleadow, A. J. W., Duddy, I. R., Green, P. F., and Hegarty, K. A. (1986b). Fission Track Lengths in the Apatite Annealing Zone and the Interpretation of Mixed Ages. *Earth Planet. Sci. Lett.* 78, 245–254. doi:10.1016/0012-821x(86)90065-8

Gleadow, A. J. W., Duddy, I. R., Green, P. F., and Lovering, J. F. (1986a). Confined Fission Track Lengths in Apatite: A Diagnostic Tool for thermal History Analysis. *Contr. Mineral. Petrol.* 94, 405–415. doi:10.1007/bf00376334

Green, P. F. (1981). A New Look at Statistics in Fission-Track Dating. *Nucl. Tracks* 5, 77–86. doi:10.1016/0191-278x(81)90029-9

Green, P. F. (1986). On the Thermo-Tectonic Evolution of Northern England: Evidence from Fission Track Analysis. *Geol. Mag.* 123, 493–506. doi:10.1017/s0016756800035081

Han, G. Q., Liu, Y. J., Li, J. J., Bai, J. Z., Sun, X. M., Wen, Q. B., et al. (2008). Uplifting Time of Huanan Uplift in the Northeastern Heilongjiang, China. *J. Jilin Univ. (Earth Sci. Ed.* 38, 389–397.

He, J. P. (2006). *The Early Cretaceous Sedimentary Characteristics and Prototype basin Restoration in Eastern Heilongjiang Province*. Dissertation/Doctor's Thesis. Changchun: Jilin University. in Chinese with English abstract.

He, Z. H., Liu, Z. J., Chen, X. Y., He, Y. P., and Chen, Y. C. (2008). Sedimentary Facies Characteristics and Their Evolution of the Early Cretaceous Relict Basins in Eastern Heilongjiang Province. *J. Palaeogeog.* 10, 151–158. in Chinese with English abstract.

He, Z. H., Liu, Z. J., Zhang, X. D., Chen, Y. H., and Dong, L. S. (2009). Subdivisions of Structural Layers and Tectonic-Sedimentary Evolution of Eastern Basins in Heilongjiang in Late Mesozoic. *World Geology.* 28, 20–27. in Chinese with English abstract.

Henry, P., Deloule, E., and Michard, A. (1996). The Erosion of the Alps: Nd Isotopic and Geothemical Constrains on the Sources of the Peri-Alpine Molasses Sediments. *Earth Planet. Sci. Let.* 146, 627–644.

Huang, Q. H., Zhang, Y., and Wang, Q. L. (1997). The Application of Fission Track Age Measurement Method in Tangyuan Rift. *Pet. Geology. Oilfield Dev. Daqing* 16, 14–16. in Chinese with English abstract. doi:10.1023/a:1018508700439

Hurford, A. J., and Green, P. F. (1983). The Zeta Age Calibration of Fission-Track Dating. *Chem. Geology.* 41, 285–317. doi:10.1016/s0009-2541(83)80026-6

Jia, C. Z., and Zheng, M. (2010). Sedimentary History, Tectonic Evolution of Cretaceous Dasanjiang basin in Northeast China and the Significance of Oil and Gas Exploration of its Residual Basins. *J. Daqing Pet. Inst.* 34, 1–12. in Chinese with English abstract.

Ketcham, R. A., Donelick, R. A., and Donelick, M. B. (2005). 11. Forward and Inverse Modeling of Low-Temperature Thermochronometry Data. *Rev. Mineral. Geochem.* 58, 275–314. doi:10.1515/9781501509575-013

Ketcham, R. A., Donelick, R. A., and Donelick, M. B. (2000). AFT Solve: a Program for Multi-Kinetic Modeling of Apatite Fission-Track Data. *Geol. Mater. Res.* 2, 1–32.

Li, G., and Yang, Q. (2003). Confirmation of an Early Cretaceous Age for the Qihulin Formation in Eastern Heilongjiang Province, China: Constraints from a New Discovery of Radiolarians. *Cretaceous Res.* 24, 691–696. doi:10.1016/j.cretres.2003.07.004

Li, J. Y., Liu, J. F., Qu, J. F., Zheng, R. G., Zhao, S., Zhang, J., et al. (2019). Major Geological Features and Crustal Tectonic Framework of Northeast china. *Acta Petrol. Sin.* 35 (10), 2989–3016. (in Chinese).

Li, Y. C., Yang, X. P., Zhou, X. F., and Wang, H. J. (2006). Integrated Straitgraphic Correlation of the Jixi Group and Longzhaogou Group in Eastern Heilongjiang. *Geology. China* 33, 1312–1320. (in Chinese with English abstract).

Liu, H. F., Liang, H. S., Li, X. Q., Yin, J. Y., Zhu, D. F., and Liu, L. Q. (2000). The Coupling Mechanisms of Mesozoic-Cenozoic Rift Basins and Extensional Mountain System in Eastern China. *Earth Sci. Front.* 7 (4), 477–486. (in Chinese with English abstract).

Liu, Z. H., Zhou, F., Wu, X. M., Sun, X. M., Zhao, C. X., Mei, M., et al. (2011). Coupling of Jiamusi Uplifting and Surrounding Mesozoic-Cenozoic Basins in Northeast China. *J. Jilin Univ.(Earth Sci. Ed.* 41 (5), 1335–1344. (in Chinese with English abstract).

Maruyama, S., Isozaki, Y., Kimura, G., and Terabayashi, M. (1997). Paleogeographic Maps of the Japanese Islands: Plate Tectonic Synthesis from 750 Ma to the Present. *Isl. Arc* 6, 121–142. doi:10.1111/j.1440-1738.1997.tb00043.x

Meng, Q. L. (2007). *Study on basin Numerical Simulation and It's Geological Significance in the Eastern Peripheral Basins of the Daqing Exploration Area*. dissertation/master's thesis. Changchun: Jilin University. (in Chinese with English abstract).

Molnar, P., and Stock, J. M. (2009). Slowing of India's Convergence with Eurasia since 20 Ma and its Implications for Tibetan Mantle Dynamics. *Tectonics* 28 (3), TC3001–TC3011. doi:10.1029/2008tc002271

Northrup, C. J., Royden, L. H., and Burchfiel, B. C. (1995). Motion of the Pacific Plate Relative to Eurasia and its Potential Relation to Cenozoic Extension along the Eastern Margin of Eurasia. *Geol* 23, 719–722. doi:10.1130/0091-7613(1995)023<0719:motppr>2.3.co;2

Ren, F. H., Yang, X. P., Li, Y. C., Wang, Y., and Zhou, X. F. (2005). Chronostratigraphic Division of the Jixi Group in Eastern Heilongjiang Province and its Geological Significance. *Geology. China* 32, 48–54. (in Chinese with English abstract).

Ren, J. S., Niu, B. G., and Liu, Z. G. (1999). Soft Collision, Superposition Orogeny and Polycyclic Suturing. *Earth Sci. Front.* 6, 85–93. (in Chinese with English abstract).

Ren, J., Tamaki, K., Li, S., and Junxia, Z. (2002). Late Mesozoic and Cenozoic Rifting and its Dynamic Setting in Eastern China and Adjacent Areas. *Tectonophysics* 344, 175–205. doi:10.1016/s0040-1951(01)00271-2

Ren, J. Y. (2018). Genetic Dynamics of China Offshore Cenozoic Basins. *Earth Sci.* 43 (10), 3337–3361. (in Chinese with English abstract).

Safonova, I. Y., Utsunomiya, A., Kojima, S., Nakae, S., Tomurtogoo, O., Filippov, A. N., et al. (2009). Pacific Superplume-Related Oceanic Basalts Hosted by Accretionary Complexes of Central Asia, Russian Far East and Japan[J]. *Gondwana Res.* 16 (3-4), 587–608. doi:10.1016/j.gr.2009.02.008

Sha, J. G. (2002). Major Achievements in Studying the Early Cretaceous Biostratigraphy of Eastern Heilongjiang. *Earth Sci. Front.* 9, 95–101. (in Chinese with English abstract).

Shi, F., Zhang, X. R., and Liu, Z. J. (2008). Thrust Event of the Provenances Revealed by Zircon Fission Track Ages in Tangyuan Fault-Basin, NE China. *Radiat. Meas.* 43, 324–328. doi:10.1016/j.radmeas.2008.04.079

Song, Y., Stepashko, A. A., and Ren, J. (2015). The Cretaceous climax of Compression in Eastern Asia: Age 87-89 Ma (Late Turonian/Coniacian), Pacific Cause, continental Consequences. *Cretaceous Res.* 55, 262–284. doi:10.1016/j.cretres.2015.01.002

Sun, G., and Dilcher, D. L. (2002). Early Angiosperms from the Lower Cretaceous of Jixi, Eastern Heilongjiang, China. *Rev. Palaeobotany Palynology* 121, 91–112. doi:10.1016/s0034-6667(02)00083-0

Sun, M.-D., Chen, H.-L., Zhang, F.-Q., Wilde, S. A., Dong, C.-W., and Yang, S.-F. (2013). A 100Ma Bimodal Composite Dyke Complex in the Jiamusi Block, NE China: An Indication for Lithospheric Extension Driven by Paleo-Pacific Roll-Back. *Lithos* 162-163 (Complete), 317–330. doi:10.1016/j.lithos.2012.11.021

Sun, W. D., Ling, M. M., Wang, F. Y., Ding, X., Hu, Y. H., Zhou, J. B., et al. (2008). Pacific Plate Subduction and Mesozoic Geological Event in Eastern China. *Bull. Mineral. Petrol. Geochem.* 27, 218–225. (in Chinese with English abstract).

Tian, Y., Ma, J. C., Liu, C., Feng, X., Liu, T. T., Zhu, H. X., et al. (2019). Effects of Subduction of the Western Pacific Plate on Tectonic Evolution of Northeast China and Geodynamic Implications. *Chin. J. Geophys.* 62 (3), 1071–1082. (in Chinese).

Uchimura, H., Kono, M., Tsunakawa, H., Kimura, G., Wei, Q., Hao, T., et al. (1996). Paleomagnetism of Late Mesozoic Rocks from Northeastern China: the Role of the Tan-Lu Fault in the North China Block. *Tectonophysics* 262, 301–319. doi:10.1016/0040-1951(96)00016-9

Wang, S., Ren, J. Y., Zhang, Y. P., Zhao, X. Q., and Yang, C. Z. (2012). Provenance Analysis of Chengzihe and Muling Formation in Jixi basin, Northeastern China. *Acta Sedimentol. Sin.* 30, 661–671. (in Chinese with English abstract).

Wen, Q. B., Liu, Y. J., Li, J. J., Bai, J. Z., Sun, X. M., Zhao, Y. L., et al. (2008). Provenance Analysis and Tectonic Implications for the Cretaceous Sandstones in the Jixi and Boli Basins, Heilongjiang. *Sediment. Geology. Tethyan Geology.* 28, 52–59. (in Chinese with English abstract).

Wu, F. Y., Ge, W. C., Sun, D. Y., and Guo, C. L. (2003). Discussions on the Lithospheric Thinning in Eastern China. *Earth Sci. Front.* 10, 51–60. (in Chinese with English abstract).

Wu, G. Z., Liu, A., Guo, X. Y., and Wu, S. M. (2007). Tectonic Subsidence History of the Suibin Depression, Sanjing basin in Heilongjiang Province. *Geotectonica et Metallogenia* 31, 412–417. (in Chinese with English abstract).

Wu, H. Y., Wang, S. H., Yang, J. G., Tang, Z. H., Wang, Z. J., and Zhang, Q. S. (2004). Analysis of Exploration Potential in Surrounding Basins of Daqing Oilfield. *China Petrol. Explor.* 2004, 23–30. (in Chinese with English abstract).

Xu, H. L., Fan, C. Y., and Gao, X. (2013). Early Cretaceous Prototype Restoration of the basin Group in Eastern Jilin. *World Geology.* 32, 263–272. (in Chinese with English abstract). doi:10.3724/sp.j.1140.2012.06027

Yang, Y.-T. (2013). An Unrecognized Major Collision of the Okhotomorsk Block with East Asia during the Late Cretaceous, Constraints on the Plate Reorganization of the Northwest Pacific. *Earth-Science Rev.* 126, 96–115. doi:10.1016/j.earscirev.2013.07.010

Yuan, W. M., Hou, Z. Q., Li, S. R., and Wang, S. C. (2001). Fission Track Evidence on thermal History of Jiama Polymetallic Ore District, Tibet. *Sci. China Ser. D: Earth Sci.* 44 (1), 139–145. (in Chinese with English abstract). doi:10.1007/bf02911981

Zhang, D. F. (2019). *Cenozoic Uplift and Exhumation Process in Sanjiang Area Heilongjiang Province*. dissertation/master's thesis. Changchun: Jilin University. (in Chinese with English abstract).

Zhang, F.-Q., Chen, H.-L., Batt, G. E., Dilek, Y., Min-Na, A., Sun, M.-D., et al. (2015). Detrital Zircon U-Pb Geochronology and Stratigraphy of the Cretaceous Sanjiang Basin in NE China: Provenance Record of an Abrupt Tectonic Switch in the Mode and Nature of the NE Asian continental Margin Evolution. *Tectonophysics* 665, 58–78. doi:10.1016/j.tecto.2015.09.028

Zhang, F.-Q., Chen, H.-L., Yang, S.-F., Feng, Z.-Q., Wu, H.-Y., Batt, G. E., et al. (2012). Late Mesozoic-Cenozoic Evolution of the Sanjiang Basin in NE China and its Tectonic Implications for the West Pacific continental Margin. *J. Asian Earth Sci.* 49, 287–299. doi:10.1016/j.jseaes.2011.12.017

Zhang, F.-Q., Dilek, Y., Chen, H.-L., Yang, S.-F., and Meng, Q.-A. (2017). Structural Architecture and Stratigraphic Record of Late Mesozoic Sedimentary Basins in NE China: Tectonic Archives of the Late Cretaceous continental Margin Evolution in East Asia. *Earth-Science Rev.* 171, 598–620. doi:10.1016/j.earscirev.2017.05.015

Zhang, F. Q., Chen, H. L., Yu, X., Dong, C. W., Yang, S. F., Pang, Y. M., et al. (2011). Early Cretaceous Volcanism in the Northern Songliao Basin, NE China, and its Geodynamic Implication. *Gondwana Res.* 19, 163–176. doi:10.1016/j.gr.2010.03.011

Zhang, Q. L., Wang, L. S., Xie, G. A., Du, J. M., Xu, S. Y., and Hu, X. Z. (2005). Discussion on Northward Extension of the Tanlu Fault Zone and its Tectonic Regime Transformation. *Geol. J. China Univ.* 11, 577–584. (in Chinese with English abstract).

Zhang, S. H., and Shi, Y. S. (1992). Paleomagnetism of Terranes in Eastern Heilongjiang Province. *J. Nanjing Univ. (Nat. Sci. Ed.* 28, 297–301. (in Chinese with English abstract).

Zhang, X. Z., Guo, Y., Zeng, Z., Fu, Q. L., and Pu, J. B. (2015). Dynamic Evolution of the Mesozoic - Cenozoic Basins in the Northeastern China. *Earth Sci. Front.* 22 (3), 88–98.

Zhang, X. Z., and Ma, Z. H. (2010). Evolution of Mesozoic-Cenozoic Basins in the Eastern Heilongjiang Province, Northeast China. *Geology. Resour* 19, 191–196. (in Chinese with English abstract).

Zhang, Y. P., Ren, J. Y., Hou, Y. P., and Yang, C. Z. (2011). Heavy mineral Characteristics and Provenance Analysis of Chengzihe and Muling Formations in Dasanjiang basin Group, East Heilongjiang Province. *Acta Petrol. Miner.* 30, 674–682. (in Chinese with English abstract).

Zhang, Y. P., Ren, J. Y., Wang, S., and Zhao, X. Q. (2016). The Sedimentary Evidence for the Existence of Unified basin in Early Cretaceous in Dasanjiang basin Group, Northeast China. *Geology. China* 43, 1280–1290. (in Chinese with English abstract).

Zhang, Y. P., Ren, J. Y., Zhao, X. Q., Tang, Y., Wang, S., and Yang, C. Z. (2012). Genesis and Significance of Conglomerate in Lower Cretaceous Muling Formation of Linkou Area, Heilongjiang Province. *Geol. Bul. China* 31, 1731–1738. (in Chinese with English abstract).

Zhang, Y. Q., Zhao, Y., Dong, S. W., and Yang, N. (2004). Tectonic Evolution Stages of the Early Cretaceous Rift Basins in Eastern China and Adjacent Areas and Their Geodynamic Background. *Earth Sci. Front.* 11 (3), 123–133. (in Chinese with English abstract).

Zhao, X. Q., Yang, S. F., Chen, H. L., Zhang, F. Q., Zhang, Y. P., Yang, C. Z., et al. (2012). Features of Multistage Cretaceous Conglomerate Deposition and its Palaeogeographic Significance in Jixi Basin of Eastern Heilongjiang, NE China. *Acta Scientiarum Naturalium Universitatis Pekinensis* 48, 419–432. (in Chinese with English abstract).

Zhao, Y., Ma, X. H., and Yang, Z. Y. (1994). Geotectonic Transition from Paleoasian System and Paleotethyan System to Paleopacific Active continental Margin in Eastern Asia. *Sci. Geol. Sin.* 29, 105–119. (in Chinese with English abstract).

Zhao, Y. (2020). *Research on the Uplift and Denudation Process since the Late Cretaceous in Huanan Area, East of Heilongjiang Province, China*. dissertation/master's thesis. Changchun: Jilin University. (in Chinese with English abstract).

Zheng, Y. D., Davis, G. A., Wang, Z., Darby, B. J., and Hua, Y. G. (1998). Large Thrust Nappe Structure in Mount Daqing, Inner Mongolia. *Sci. China (Ser. D)* 28, 289–295. (in Chinese with English abstract).

Zhou, D., Ru, K., and Chen, H. Z. (1995). Kinematics of Cenozoic Extension on the south china Sea continental Margin and its Implications for the Tectonic Evolution of the Region. *Tectonophysics* 251 (1-4), 161–177. doi:10.1016/0040-1951(95)00018-6

Zhou, J.-B., and Wilde, S. A. (2013). The Crustal Accretion History and Tectonic Evolution of the NE China Segment of the Central Asian Orogenic Belt. *Gondwana Res.* 23 (4), 1365–1377. doi:10.1016/j.gr.2012.05.012

Zhou, J.-B., Wilde, S. A., Zhang, X.-Z., Zhao, G.-C., Zheng, C.-Q., Wang, Y.-J., et al. (2009). The Onset of Pacific Margin Accretion in NE China: Evidence from the Heilongjiang High-Pressure Metamorphic belt. *Tectonophysics* 478, 230–246. doi:10.1016/j.tecto.2009.08.009

Zhou, J. P., Dunkl, I., Liu, W. M., and Eynatten, H. V. (2020). Late Cretaceous-Tertiary Tectonic Inversion of Northeastern Asian continental Margin: Insight from the Low Temperature Thermochronology in NE China, Preprint. *Gondwana Res.* Available at:. doi:10.1016/j.gr.2020.05.017

Zhu, G., Wang, D. X., Liu, G. S., Niu, M. L., and Song, C. Z. (2004). Evolution of the Tan-Lu Fault Zone and its Responses to Plate Movements in West pacific basin. *Sci. Geol. Sin.* 39 (1), 36–49. (in Chinese with English abstract).

Conflict of Interest: The authors declare that the research was conducted in the absence of any commercial or financial relationships that could be construed as a potential conflict of interest.